Energy Fuels **2010,** *24,* 1552–1558 · DOI:10.1021/ef901171k
Published on Web 01/07/2010

energy&fuels
article

Numerical Study of Inhibition of Hydrogen/Air Flames by Atomic Iron

Vladimir M. Shvartsberg,* Tatyana A. Bolshova, and Oleg P. Korobeinichev

Institute of Chemical Kinetics and Combustion, Novosibirsk 630090, Russia

Received October 14, 2009. Revised Manuscript Received December 18, 2009

The inhibition of laminar premixed H_2/air flames by atomic iron was studied for various equivalence ratios using numerical methods. The inhibition effectiveness was shown to strongly depend upon the equivalence ratio, with the minimum effectiveness being observed at $\phi \approx 2$. Calculations of the recombination rates of H and O atoms and OH radicals in reactions involving iron-containing species revealed the causes of the higher inhibition effectiveness in lean and near-stoichiometric ($\phi < 2$) and rich ($\phi > 2$) flames. The higher inhibition effectiveness in lean flames is due to the optimal composition of iron-containing combustion products, resulting in a high recombination rate of active flame species. Increased inhibition effectiveness in rich flames is due to a low rate of chain branching under fuel-rich conditions rather than a high rate of active species removal from the flame zone.

1. Introduction

The first studies of iron-containing species (ICS) as flame inhibitors were performed in the early 1960s.[1,2] Lask and Wagner[1] were the first to measure the effect of iron pentacarbonyl $Fe(CO)_5$ on the speed of H_2/air and CH_4/air flames and show that it was 2 orders of magnitude greater than that of CF_3Br. Miller et al.[2] studied the effect of some inhibitors, including $Fe(CO)_5$, on the speed of H_2/air flames for various equivalence ratios (ϕ) and an inhibitor concentration of 0.5% by volume. Unfortunately, the addition of $Fe(CO)_5$ at this concentration greatly changed the equivalence ratio of the initial flame because 2.5% by volume of carbon monoxide was also added to the flame and the effect as a result of iron alone was difficult to assess. Later, Vanpee and Shirodkar[3] studied a wide range of metal-containing compounds as flame inhibitors and compared their effectiveness.

An increased interest in metal-containing compounds, including iron pentacarbonyl and ferrocene $Fe(C_6H_6)_2$ as flame inhibitors, has arisen after the ban on the production of halogenated fire-extinguishing agents (such as CF_3Br) with a high ozone depletion potential. Searches for new inhibitors and fire suppressants have led scientists to pay attention to ICS compounds. Reinelt and Linteris[4] studied the effect of $Fe(CO)_5$ and ferrocene on premixed laminar flame speeds and extinction strain rates of opposed-jet diffusion flames. The inhibition effectiveness was shown to strongly depend upon the dopant loading; the maximum inhibition was achieved at a concentration as low as 100 μL/L (μL/L is equivalent to parts per million by volume) and was then little affected by a further increase in the concentration. The authors of ref 4 attribute this to the formation of iron-containing particles in the flame, resulting in a reduction in the gas-phase concentration of iron species (which are responsible for flame inhibition). According to data,[4] an increase in the oxygen volume fraction in a $O_2 + N_2$ mixture reduces the inhibition effect. This may be due to the combustibility of iron pentacarbonyl and ferrocene.

Linteris et al.[5] performed experimental and modeling studies of the effect of $Fe(CO)_5$ and $Fe(C_6H_6)_2$ additives on the speed of a $CH_4/O_2/N_2$ flame. The numerical study was based on a kinetic model,[6] which provided a good fit to experimental results. Ferrocene, whose molecule contains more fuel than that of iron pentacarbonyl, showed a lower inhibition effect than $Fe(CO)_5$.

Rumminger et al.[6] determined the key chemical processes responsible for flame inhibition

$$FeOH + H = FeO + H_2$$

$$FeO + H_2O = Fe(OH)_2$$

$$Fe(OH)_2 + H = FeOH + H_2O$$

This is equivalent to the recombination of hydrogen atoms $H + H = H_2$. The catalytic recombination of O atoms also involves three elementary reactions

$$Fe + O_2 + M = FeO_2 + M$$

$$FeO_2 + O = FeO + O_2$$

$$FeO + O = Fe + O_2$$

The role of the formation of iron-containing particles in the inhibition of hydrogen and methane flames by a $Fe(CO)_5$ additive was studied in refs 7 and 8. The results showed that the formation of iron particles reduced the inhibition effect of the iron pentacarbonyl additive. This supports

*To whom correspondence should be addressed. Telephone: +7-(383)-333-33-46. Fax: +7-(383)-330-73-50. E-mail: vshvarts@kinetics.nsc.ru.

(1) Lask, G.; Wagner, H. G. *Proc. Combust. Inst.* **1962**, *8*, 432–438.
(2) Miller, D. R.; Evers, R. L.; Skinner, G. B. *Combust. Flame* **1963**, *7*, 137–142.
(3) Vanpee, M.; Shirodkar, P. *Proc. Combust. Inst.* **1979**, *18*, 787–793.
(4) Reinelt, D.; Linteris, G. T. *Proc. Combust. Inst.* **1996**, *26*, 1421–1428.
(5) Linteris, G. T.; Rumminger, M. D.; Babushok, V. I.; Tsang, W. *Proc. Combust. Inst.* **2000**, *28*, 2965–2972.
(6) Rumminger, M. D.; Reinelt, D.; Babushok, V. I.; Linteris, G. T. *Combust. Flame* **1999**, *116*, 207–219.
(7) Rumminger, M. D.; Linteris, G. T. *Combust. Flame* **2000**, *123*, 82–94.
(8) Rumminger, M. D.; Linteris, G. T. *Combust. Flame* **2002**, *128*, 145–164.

the hypothesis[4] of a gas-phase mechanism for flame inhibition by ICS.

Experimental studies of cup-burner flame suppression by metallic compounds[9] have provided further evidence for the gas-phase mechanism of inhibition by ICS. Models ignoring solid-phase formation in flame predict the greater inhibition effect than experimental data.

Recently, Linteris and Babushok[10] presented interesting numerical results on the auto-ignition of lean ($\phi = 0.15$) and stoichiometric H_2/air mixtures in the presence of iron pentacarbonyl and other iron compounds. They found that the auto-ignition delay decreased by a factor of 2−3 at a loading of 50 μL/L; i.e., iron compounds promoted auto-ignition. At a slightly higher volume fraction (> 150 μL/L), ignition was retarded. The authors explain the promotion effect by the formation of O atoms by the reaction $FeO + O_2 = FeO_2 + O$ under fuel-lean conditions. Atomic oxygen then reacts with H_2 to produce H + OH, resulting in an increase in the chain-carrier concentration and, hence, in the promotion of auto-ignition. The inhibition observed at higher concentrations of iron compounds in this system is due to the cyclic recombination of radicals.

Rubtsov et al.[11] observed a promotion of auto-ignition and combustion of a H_2/O_2 mixture by the addition of chromium and molybdenum pentacarbonyl at low pressure. The authors may improperly explain the observed effect by radical recombination on the surface of the particles consisting of oxidation products of the dopants.

Spatial variations in the temperature and concentration of atomic iron in a low-pressure lean ($\phi = 0.37$) $H_2/O_2/Ar/Fe(CO)_5$ flame were measured using laser-induced fluorescence.[12,13] Iron pentacarbonyl was found to decompose in the flame to produce atomic iron, which was then transformed to iron oxides and hydroxides. On the basis of a previously developed mechanism,[6] a reduced 12-step mechanism for flame inhibition by $Fe(CO)_5$ was developed and validated by comparing measured and simulated concentration profiles of atomic iron.

A low-pressure, rich ($\phi = 2.3$), laminar, premixed propene/oxygen/argon flame doped with ferrocene was studied experimentally using molecular beam mass spectrometry (MBMS) and laser-induced fluorescence (LIF) and by numerical simulations.[14] The flame temperature was obtained by two-line OH LIF measurements, and the additive was found to increase the postflame temperature by 40 K. MBMS analysis of the species profiles of important intermediates in flames with and without ferrocene doping showed a slight increase in the maximum concentration of species, such as CH_2O, C_5H_5, and C_6H_6. At the same time, the dopant slightly decreased the maximum concentration of the propargyl radical C_3H_3, which is known to be an intermediate in the formation of soot precursors. The MBMS measurements showed that the flame velocity decreased with the addition of ferrocene, which was not predicted by the model.

Staude and Atakan[15] carried out equilibrium calculations for iron-doped hydrogen/oxygen/argon and propene/oxygen/argon gas mixtures under combustion-relevant conditions. It is noteworthy that condensed Fe-containing compounds were considered in the calculations. The focus was on iron intermediates and the conditions under which condensed phases of iron or iron species could be expected in the flame. The stoichiometry (ϕ = 0.37, 1, and 2.3), temperature (1000−2500 K), and pressure (0.03−1 bar) were varied, allowing for a prediction of which gas-phase iron species might be expected in measurable concentrations under the flame conditions used. The effect of the sampling probe on the composition of the combustion products, which are cooled during probing, was discussed.

The present work extends previous studies by other authors of atmospheric-pressure iron-doped H_2/air flames. The work is focused on the causes of significant differences in the degree of inhibition and combustion chemistry in flames with different equivalence ratios.

2. Modeling Approach

The speed and structure of H_2/air flames doped with atomic iron at a pressure of 0.1 MPa were simulated using mechanisms for hydrogen oxidation[16] and flame inhibition by ICS.[6] Atomic iron was used as a dopant, and the decomposition of iron pentacarbonyl and CO oxidation were eliminated from the kinetic model. Thus, the influence of carbon monoxide on inhibition was not taken into account.

Spatial variations in the rates of production of chain carriers via reactions involving ICS in the flames were calculated using the KINALC code,[17] a postprocessor of the output files of the PREMIX code.[18,19] Because the reaction mechanism used in the calculations contained only irreversible reactions, the original mechanisms[6,13] were first converted to an irreversible form by the MECHMOD code.[20] We note that, although the production rate via particular reactions was calculated by irreversible reactions, below it is given as a net reaction rate for the reversible reaction.

Windward differencing was used, and the grid was refined to GRAD = 0.1 and CURV < 0.2 (parameters controlling the number of grid points inserted in regions of high gradient and high curvature in the PREMIX code). These values of GRAD and CURV provided a sufficient refinement of the grid, so that the flame speed was independent of the number of grid points (≈200−250 required). In all calculations, the energy equation was solved and mixture-averaged and thermal diffusions were used.

3. Results and Discussion

3.1. Effect of Iron on the Flame Speed. Figure 1 shows speeds of H_2/air flames without additive and those doped

(9) Linteris, G. T.; Katta, V. R.; Takahashi, F. *Combust. Flame* **2004**, *138*, 78–96.
(10) Linteris, G. T.; Babushok, V. I. *Proc. Combust. Inst.* **2009**, *32*, 2535–2542.
(11) Rubtsov, N. M.; Chernysh, V. I.; Tsvetkov, G. I.; Seplyarskii, B. S. *Mendeleev Commun.* **2006**, *16* (5), 282–284.
(12) Wlokas, I.; Staude, S.; Hecht, C.; Atakan, B.; Schulz, C. Measurement and simulation of Fe-atom concentration in premixed $Fe(CO)_5$-doped low-pressure H_2/O_2 flames. Proceedings of the European Combustion Meeting, Vienna, Austria, 2009.
(13) Staude, S.; Hecht, C.; Wlokas, I.; Schulz, C.; Atakan, B. *Z. Phys. Chem.* **2009**, *223*, 639–649.
(14) Tian, K.; Li, Z. S.; Staude, S.; Li, B.; Sun, Z. W.; Lantz, A.; Alden, M.; Atakan, B. *Proc. Combust. Inst.* **2009**, *32*, 445–452.
(15) Staude, S.; Atakan, B. *Open Thermodyn. J.* **2009**, *3*, 42–46.
(16) Conaire, M. O.; Curran, H. J.; Simmie, J. M.; Pitz, W. J.; Westbrook, C. K. *Int. J. Chem. Kinet.* **2004**, *36* (11), 603–622.
(17) Turanyi, T.; Zsely, I. G.; Frouzakis, C. KINALC: A CHEMKIN based program for kinetic analysis (available at http://www.chem.leeds.ac.uk/Combustion/Combustion.html).
(18) Kee, R. J.; Grcar, J. F.; Smooke, M. D.; Miller, J. A. A program for modeling steady, laminar, one-dimensional premixed flames. Report SAND85-8240, Sandia National Laboratories, Albuquerque, NM, 1985.
(19) Kee, R. J.; Rupley, F. M.; Miller, J. A. Chemkin II: A Fortran chemical kinetics package for the analysis of gas-phase chemical kinetics. Report SAND89-8009, Sandia National Laboratories, Albuquerque, NM, 1989.
(20) Turanyi, T. Mechmod version 1.4: Program for the transformation of kinetic mechanisms (available at http://www.chem.leeds.ac.uk/Combustion/Combustion.html).

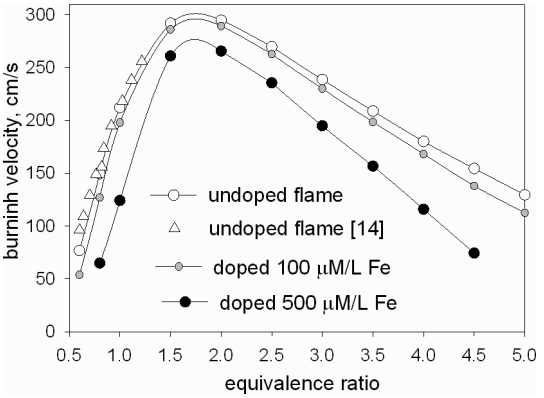

Figure 1. Speed of H_2/air flames without additives and doped with 100 and 500 μL/L atomic iron versus the equivalence ratio at a pressure of 0.1 MPa. Lines, modeling results; symbols, experimental data.[14]

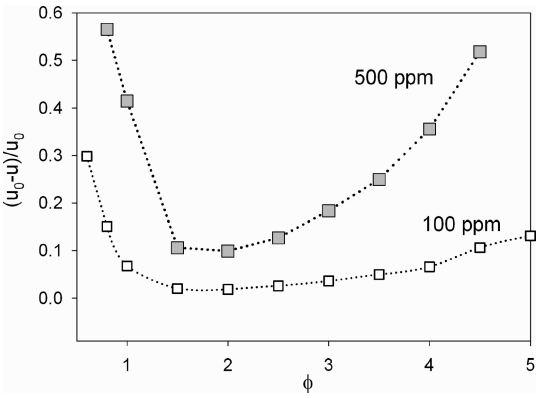

Figure 2. Inhibition effectiveness of atmospheric-pressure H_2/air flames doped with 100 and 500 μL/L atomic iron, expressed as the relative decrease in the flame speed because of inhibitor addition $(u_0 - u)/u_0$ versus the equivalence ratio.

with 100 and 500 μL/L atomic iron at a pressure of 0.1 MPa versus the equivalence ratio. In addition, Figure 1 gives experimental speeds of the undoped flames.[21] Good agreement between the reference experimental and modeling results confirms the validity of the chosen mechanism for the conditions considered. The modeling results show that the inhibition intensity depends upon ϕ of unburnt gases.

Figure 2 shows the inhibition effectiveness expressed as the relative decrease in the flame speed because of inhibitor addition ($F = (u_0 - u)/u_0$, where u_0 is the speed of the undoped flame and u is the speed of the Fe-doped flame) versus ϕ. The effectiveness was calculated for inhibitor concentrations of 100 and 500 μL/L because, at a low concentration, the thermal properties of the inhibitor make a minor contribution to its total effect and its chemical activity becomes more evident.[22]

It is evident from Figure 2 that the minimum inhibition effectiveness is observed at $\phi \approx 2$ for both iron loadings. The inhibition effectiveness increases as the unburnt gas composition changes, with the increase being greater in lean than in rich flames. This effect is especially pronounced for flames

(21) Egolfopoulos, F. N.; Law, C. K. *Proc. Combust. Inst.* **1990**, *23*, 333–340.

(22) Zamashchikov, V. V.; Bunev, V. A. *Combust. Explos. Shock Waves* **2001**, *37* (4), 378–386.

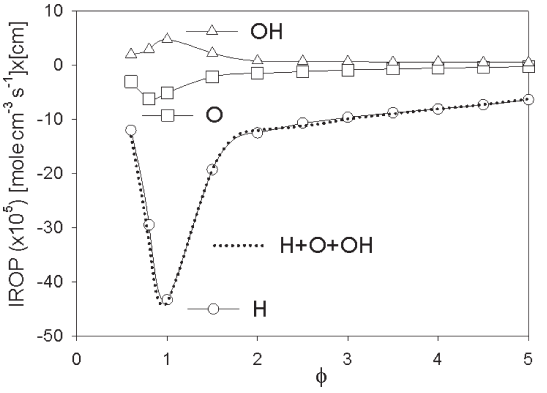

Figure 3. Integrated production rate (mol cm^{-3} s^{-1}) × (cm) of H, O, and OH and the total production rate of all of these species in reactions involving ICS in atmospheric-pressure H_2/air flames doped with 100 μL/L atomic iron versus the equivalence ratio.

with the minimum loading, for which modeling was performed over a wider range of equivalence ratios.

It is well-known that flame inhibition by ICS as well as other chemically active inhibitors is due to the removal of active chain carriers from the flame via catalytic recombination reactions. To understand the causes of different inhibition effectiveness of flames with different ϕ, we calculated the spatial variation (along the flame zone) in the rate of production of the active flame species H, O, and OH in reactions involving ICS for all flames studied. However, a quantitative comparison of these profiles (summarized over all reactions) in different flames is practically impossible because they all have different shapes, widths, and magnitudes. For comparison and quantitative evaluation of the inhibitor effect on active flame species, we used integrals of the rate-of-production profiles with respect to the distance transverse to the flame front. The limits of integration covered only the reaction zone of the flame and not the entire flame zone because the inhibition effectiveness is mainly related to the radical scavenging in the vicinity of the maximum concentration of chain carriers. The integrals were negative for H and O atoms (which were consumed in the reactions involving ICS) and positive for OH radicals (which were produced in the reactions). Thus, we can speak of the consumption rate for H and O atoms and the production rate for OH. The integrals were multiplied by 10^5 for convenience of comparison.

Figure 3 gives integrals of the production rate of H, O, and OH versus the equivalence ratio for Fe-doped flames. The results clearly show that the addition of atomic iron mainly removes H atoms and, to a lesser extent, O atoms from the flames. Furthermore, the additive provides an additional channel for OH production. The integrated production rates of O and OH are similar in magnitude but opposite in sign. The integrated production rate of H + O + OH differs only slightly from that of atomic H.

Moreover, the total integrated production rate for H + O + OH as a function of ϕ has a minimum at $\phi = 1$, as seen in Figure 3. If we assume that the inhibition effectiveness is determined only by the rate of removal of active chain carriers from the flame, then the minimum inhibition effectiveness should be observed for the leanest and richest flames. However, this assumption contradicts the modeling data given in Figure 2. This contradiction has led us to suggest that, for flames with significantly different equivalence

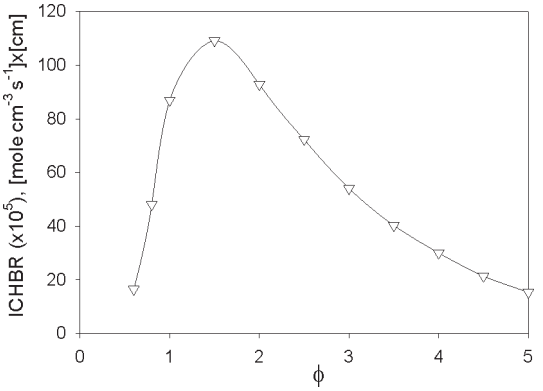

Figure 4. Integrated net reaction rate of the chain-branching reaction $H + O_2 = OH + O$ (mol cm^{-3} s^{-1}) × (cm) in atmospheric-pressure H_2/air flames doped with 100 μL/L atomic iron versus the equivalence ratio.

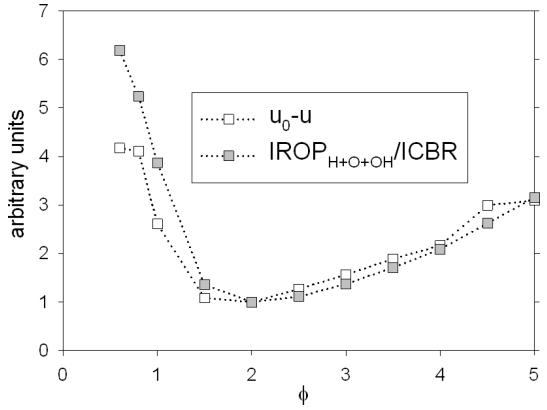

Figure 5. Inhibition effectiveness of atmospheric-pressure H_2/air flames doped with 100 μL/L atomic iron, expressed as (1) the decrease in flame speed because of doping (open symbols) and (2) the ratio of the integrated production rates of chain carriers (H + O + OH) to the chain-branching rate (gray symbols).

ratios and, hence, different flame temperatures, the inhibition effectiveness cannot be compared only on the basis of chain-termination rates. It is necessary to take into account at least one more parameter that changes with the equivalence ratio. This can be the chain-branching rate, i.e., the net rate of the reaction $H + O_2 = OH + O$, which is known to be the key process in hydrogen combustion.[23−26] Therefore, the ratio of the integrated production rate of H + O + OH to the chain-branching rate was used as a parameter that determines the inhibition effectiveness of flames over a wide range of equivalence ratios. Because the radical production and chain-branching rates vary along the flame zone, it was convenient to integrate the profiles of each of these rates and estimate the ratio of the integrals for each flame. Figure 4 gives integrals of the chain-branching rate versus the equivalence ratio. The integral of the production rate reaches a maximum at $\phi = 1.5$.

Figure 5 shows the ratio of the integral of the production rate to the integral of the chain-branching rate and the difference between the speeds of undoped and Fe-doped (100 μL/L) flames versus the equivalence ratio. For ease of comparison, each of the dependences was normalized by its minimum value (at $\phi = 2$). As seen in Figure 5, both curves are similar in shape but do not coincide quantitatively. Thus, the ratio of the radical production rate to the chain-branching rate determines the inhibition effectiveness for flames with significantly different equivalence ratios.

It is evident from the results presented above that, to explain the dependence of the inhibition effectiveness upon ϕ, it is necessary to consider the interplay of two basic processes: radical removal from the flame and chain branching, because the chain-branching rate greatly depends upon the flame temperature and, hence, the equivalence ratio. We note that an increase in the inhibition effectiveness in rich ($\phi > 2$) and lean ($\phi < 1$) flames is due to a relative decrease in the chain-branching rate rather than an increase in the rate of removal of active species. Similarly, the low inhibition effectiveness at $\phi = 2$ is explained by the relatively high rate of chain branching rather than by the low rate of active species removal. It follows from the aforesaid that the inhibition effectiveness is higher for flames in which the chain-branching rate is lower, with other things being equal.

Previously,[19] we have shown that the effectiveness of $H_2/O_2/N_2$ flame inhibition by trimethylphosphate increases as the unburnt gases are diluted with N_2. We attributed this to a decrease in the flame temperature and, hence, the chain-branching rate. However, the explanation given above is more general and validated by the results of modeling and sensitivity analysis.

Table 1. Basic Reactions Involving ICS Responsible for the Consumption of H Atoms in H_2/Air Flames of $\phi = 0.6$, 1, and 5 and Their Contribution to the Total Consumption Rate C_H (Only Reactions Involving ICS Are Considered)

ϕ	reaction	C_H (%)
0.6	$Fe(OH)_2 + H = FeOH + H_2O$	57.5
	$FeOH + H = FeO + H_2$	39.4
1	$Fe(OH)_2 + H = FeOH + H_2O$	40.9
	$FeOH + H = FeO + H_2$	36.4
5	$Fe(OH)_2 + H = FeOH + H_2O$	37.8
	$FeOH + H = FeO + H_2$	39.8
	$FeO_2 + H + M = FeOOH + M$	11.7

3.2. Inhibition Chemistry. The next step in the study of the inhibition of H_2/air flames by atomic iron was to identify the chemical processes responsible for changes in the production rates of H, O, and OH as ϕ changes. The crucial reactions of H and O consumption and OH production were first identified.

Three flames were chosen for the analysis: a lean flame with $\phi = 0.6$, a stoichiometric flame with the maximum rate of radical production, and the richest flame with $\phi = 5$. The rate of H atom production in separate reactions was calculated, and the key reactions for each of the chosen flames were determined (Table 1). In addition, we calculated the contribution of each reaction to the total rate of H consumption, considering only the reactions involving ICS. The data in Table 1 indicate that, regardless of the flame equivalence ratio, the key reactions responsible for H atom removal are as follows:

$$FeOH + H = FeO + H_2 \quad (1)$$

$$Fe(OH)_2 + H = FeOH + H_2O \quad (2)$$

This was also shown previously for a stoichiometric $CH_4/O_2/N_2$ flame.[6] In the richest flame ($\phi = 5$), the reaction

(23) Westbrook, C. K.; Mizobuchi, Y.; Poinsot, T. J.; Smith, P. J.; Warnatz, J. *Proc. Combust. Inst.* **2005**, *30*, 125–157.
(24) Konnov, A. A. *Combust. Flame* **2008**, *152*, 507–528.
(25) Rumminger, M. D.; Babushok, V. I.; Linteris, G. T. *Proc. Combust. Inst.* **2002**, *29*, 329–336.
(26) Korobeinichev, O. P.; Rybitskaya, I. V.; Shmakov, F. G.; Chernov, A. A.; Bolshova, T. A.; Shvartsberg, V. M. *Proc. Combust. Inst.* **2009**, *32*, 2591–2597.

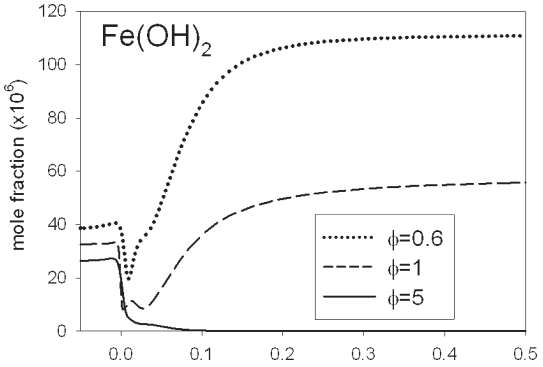

Figure 6. Simulated spatial variation of the mole fraction of $Fe(OH)_2$ in H_2/air flames with $\phi = 0.6$, 1, and 5 doped with 100 μL/L atomic iron at a pressure of 0.1 MPa.

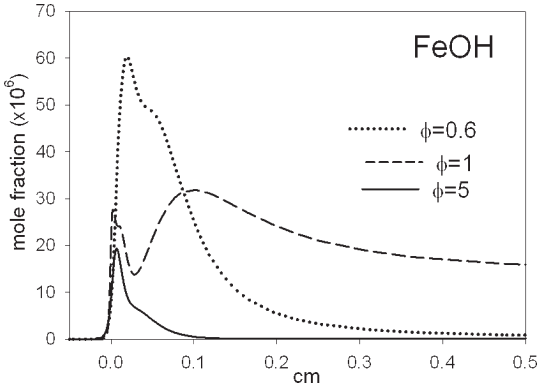

Figure 7. Simulated spatial variation of the mole fraction of FeOH in H_2/air flames with $\phi = 0.6$, 1, and 5 doped with 100 μL/L atomic iron at a pressure of 0.1 MPa.

$FeO_2 + H + M = FeOOH + M$ also makes a noticeable contribution to the removal of H atoms from the flame. Reactions 1 and 2 have relatively low activation barriers (6690 and 2510 J/mol, respectively), and the difference in the reaction rate constant between the stoichiometric flame and the rich ($\phi = 5$) flame is 20% for reaction 1 and less than 10% for reaction 2 (for these flames, the difference in the flame temperature in the zone of these reactions is about 500 K). At the same time, the H production rate in the lean and rich flames is about 7 times lower than that in the stoichiometric flame. Consequently, the difference in the production rate between the flames considered here is determined mainly by reactant concentrations and not the flame temperature.

The concentration profiles of $Fe(OH)_2$ and FeOH in the three selected flames doped with 100 μL/L atomic iron are given in Figures 6 and 7, respectively. It is evident from these profiles that the concentration of iron hydroxides in the flames decreases as the equivalence ratio increases. Figure 6 shows a noticeable level of $Fe(OH)_2$ in the unburnt gases for the mixture doped with atomic iron. This is due to the high reactivity of the dopant, as proposed in the model.[6] It reacts with the combustible mixture at room temperature to produce mainly $Fe(OH)_2$ and FeO_2 (see below). If we assume that the H consumption rate is determined only by the concentration of $Fe(OH)_2$ and FeOH, the maximum rate should be observed in the leanest flame, but this is inconsistent with the data in Figure 3. From this, it follows that the H atom concentration in the flame, which strongly depends upon ϕ, also determines the H consumption rate.

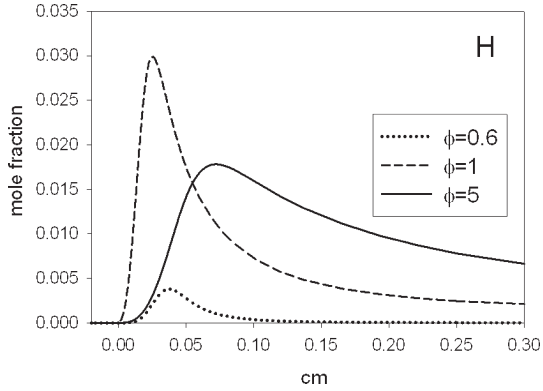

Figure 8. Simulated spatial variation of the mole fraction of H atoms in H_2/air flames with $\phi = 0.6$, 1, and 5 doped with 100 μL/L atomic iron at a pressure of 0.1 MPa.

Table 2. Basic Reactions Involving ICS Responsible for the Consumption of O Atoms in H_2/Air Flames of $\phi = 0.6$, 1, and 5 and Their Contribution to the Total Consumption Rate C_O (Only Reactions Involving ICS Are Considered)

ϕ	reaction	C_O (%)
0.6	$FeOH + O = FeO + OH$	49.4
	$FeO_2 + O = FeO + O_2$	21.3
	$Fe + O_2 = FeO + O$	10.6
1	$FeOH + O = FeO + OH$	19.5
	$FeO_2 + O = FeO + O_2$	44.6
	$Fe + O_2 = FeO + O$	26.4
5	$FeOH + O = FeO + OH$	2.0
	$FeO_2 + O = FeO + O_2$	95.6
	$Fe + O_2 = FeO + O$	1.5

Figure 8 gives concentration profiles of the H atom in the three selected flames doped with 100 μL/L atomic iron. A comparison of the H concentrations shows that, although the concentration of iron hydroxides in the lean ($\phi = 0.6$) flame is 2 times higher than that in the stoichiometric flame, the H production rate is higher in the stoichiometric flame because the H concentration in this flame is 7 times higher than that in the lean flame.

In $H_2/O_2/N_2$ flames doped with 100 μL/L atomic iron, O atoms were found to be consumed mainly in the following reactions:

$$FeOH + O = FeO + OH \quad (3)$$

$$FeO_2 + O = FeO + O_2 \quad (4)$$

$$Fe + O_2 = FeO + O \quad (5)$$

Although reaction 3 is a key reaction of O atoms consumption, it is unlikely to contribute to the inhibition effectiveness because it transforms one chain carrier to another (O → OH). This fact largely determines the symmetry of the O and OH curves in Figure 3. The activation energies of these reactions do not exceed 6500 J/mol, and the temperature influence on the rate of this reaction can therefore be ignored. The contribution of each of these reactions to the total production rate varies with the flame equivalence ratio (Table 2). In the lean flame, reaction 3 plays a crucial role in the removal of O atoms because of the high concentration of FeOH in this flame (Figure 7). In the stoichiometric flame, this process is determined by reaction 4 because of the relatively high concentration of FeO_2 (Figure 9) and the high concentration of O atoms (Figure 10). Reaction 5 (proceeding in the reverse direction) is important for the removal of O atoms from the

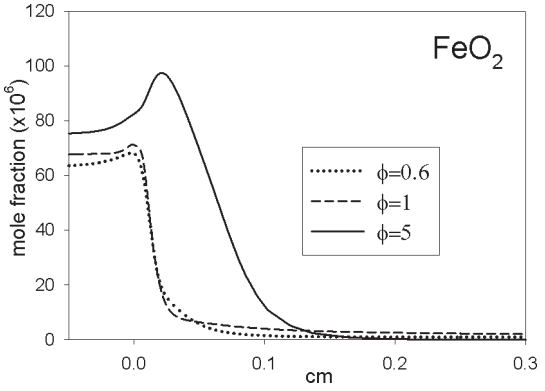

Figure 9. Simulated spatial variation of the mole fraction of FeO_2 in H_2/air flames with $\phi = 0.6$, 1, and 5 doped with 100 μL/L atomic iron at a pressure of 0.1 MPa.

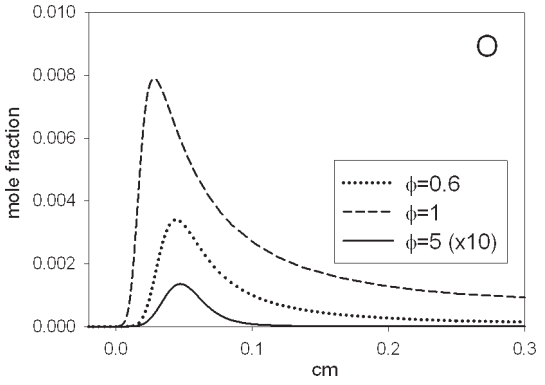

Figure 10. Simulated spatial variation of the mole fraction of O atoms in H_2/air flames with $\phi = 0.6$, 1, and 5 doped with 100 μL/L atomic iron at a pressure of 0.1 MPa.

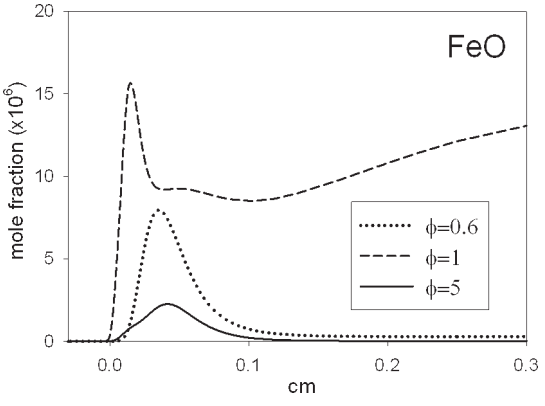

Figure 11. Simulated spatial variation of the mole fraction of FeO in H_2/air flames with $\phi = 0.6$, 1, and 5 doped with 100 μL/L atomic iron at a pressure of 0.1 MPa.

flames with $\phi = 0.6$ and 1 because of the higher concentration of FeO (Figure 11) in these flames; in the rich flame, this reaction plays an insignificant role, primarily because of the very low concentration of O atoms. The key role of reaction 4 in the removal of O atoms from the rich flame is due to the highest concentration of FeO_2 in this flame compared to other iron-containing products.

The maximum total rate of O removal (via all reactions involving ICS) is observed in the stoichiometric flame because of the highest concentration of FeO and considerable concentrations of other active products of atomic iron

Table 3. Basic Reactions Involving ICS Responsible for the Production of OH Radicals in H_2/Air Flames of $\phi = 0.6$, 1, and 5 and Their Contribution to the Total Consumption Rate C_{OH} (Only Reactions Involving ICS Are Considered)

ϕ	reaction	C_{OH} (%)
0.6	$FeOH + O = FeO + OH$	76.7
	$Fe(OH)_2 + OH = FeOOH + H_2O$	14.7
	$FeO + H = Fe + OH$	3.4
1	$FeOH + O = FeO + OH$	32.0
	$FeO + H = Fe + OH$	21.2
	$FeOOH + H = FeOH + OH$	1.3
5	$Fe(OH)_2 + OH = FeOOH + H_2O$	29.4
	$FeO + H = Fe + OH$	21.6
	$FeO_2 + H = FeO + OH$	19.2
	$FeOOH + H = FeOH + OH$	29.4

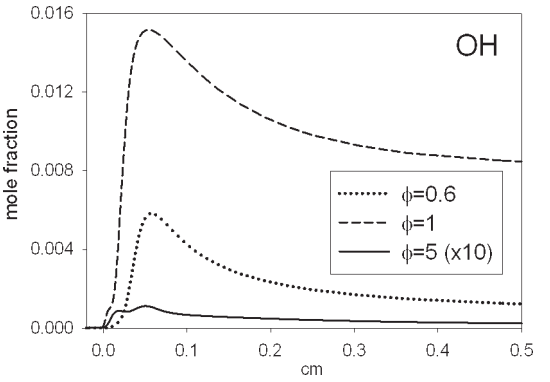

Figure 12. Simulated spatial variation of the mole fraction of OH radicals in H_2/air flames with $\phi = 0.6$, 1, and 5 doped with 100 μL/L atomic iron at a pressure of 0.1 MPa.

oxidation in this flame. In addition, another important factor responsible for the highest rate of O consumption in the stoichiometric flame is the high concentration of O atoms; it is 2 times higher than that in the lean ($\phi = 0.6$) flame and almost 60 times higher than that in the rich flame ($\phi = 5$). The O consumption rate in the rich flame is obviously very low at that low concentration of O atoms.

The key reactions of OH production involving ICS are given in Table 3. In the lean and stoichiometric flames, reaction 3 is of importance, whereas in the rich flame, it plays a minor role. The reaction $Fe(OH)_2 + OH = FeOOH + H_2O$ is given in the form proposed in the model[6] but proceeds with OH formation. The OH production rate is determined by the concentration of the following products of iron oxidation: $Fe(OH)_2$, FeOH, FeO_2, and FeO. However, the crucial factor determining the OH production rate is the strong dependence of the OH concentration upon the flame stoichiometry (Figure 12). The OH concentration in the stoichiometric flame is 2.6 times higher than that in the lean flame and almost 140 times higher than that in the rich flame.

Thus, the production rate of active species in flames doped with atomic iron is governed by two main factors: the concentration of active ICS in the reaction zone of the flame and the concentration of chain carriers in the flame.

In considering the production kinetics of chain carriers in reactions involving inhibitors, it should be kept in mind that the addition of an inhibitor to a flame also affects the rate of those reactions that do not involve the inhibitor. For example, OH production via reactions involving iron compounds does not increase the OH radical concentration in Fe-doped flames compared to the undoped flames. On the contrary, the OH concentration slightly decreases as the inhibitor is

added. This results from the effect of the inhibitor on the rate of the reactions included in the hydrogen oxidation mechanism.

4. Summary

The inhibition effect of atomic iron on H_2/air flames, expressed as the relative decrease in the flame speed as the inhibitor is added, substantially depends upon the equivalence ratio of unburnt gases. The minimum effectiveness is observed at $\phi \approx 2$, and the maximum effectiveness is observed in lean flames. The dependence of the inhibition effectiveness upon the equivalence ratio is determined not only by the chain-carrier production rate but also by the chain-branching rate, which is appreciably different in flames with different stoichiometry.

The products of atomic iron oxidation in H_2/air flames mainly catalyze H atom recombination, and the recombination rate is largely determined by the concentration of iron hydroxides FeOH and $Fe(OH)_2$. The O atom recombination rate depends upon the concentration of iron-containing flame species and, to a large extent, the O atom concentration in the flames.

Acknowledgment. We thank Dr. G. T. Linteris for providing the kinetic model for flame inhibition by iron pentacarbonyl.